RESEARCH ACTIVITIES VIII
Coordination Chemistry Laboratories

Prof. Hiroshi Kitagawa (Kyushu Univ.) and Assoc. Prof. Mitsuru Kondo (Shizuoka Univ.) took the position of the Laboratory of Complex Catalyst from April 2006. Prof. Kazushi Mashima (Osaka Univ.) and Assoc. Prof. Masato Kurihara (Yamagata Univ.) finished their term as Adjunct Prof. of the Laboratory of Complex Catalyst in March 2006. Their effort during their term is gratefully appreciated. Prof. Yoichi Ishii (Chuou Univ.) and Prof. Takashi Hayashi (Osaka Univ.) continue the position of Laboratory of Coordination Bond.

VIII-A Metal Complexes Aimed at Conversion between Chemical and Electrochemical Energies

Metal complexes that have an ability to oxidize organic molecules at potentials more negative than the reduction potential of dioxygen have potential uses for electro-catalysts in fuel cells. Metal–oxo complexes are possible candidates for the oxidation of organic molecules, since metal–oxo species are believed to work as active centers in various metal enzymes, which oxidize various biological substrates under very mild conditions. Mechanistic understandings of the reactivity of metal–oxo species, however, are limited due to the difficulty of preparation of reactive M–O frameworks in artificial systems. On the other hand, reactivity of high valent Ru=O complexes prepared by sequential electron and proton loss of the corresponding Ru–OH_2 ones have been extensively studied and proven to work as oxidants of organic molecules to some extent. We have succeeded reversible conversion between aqua and oxo ligands on Ru–dioxolene frameworks without using any oxidants by taking advantage of dioxolene as a redox active ligand. Along this line, we have been preparing a variety of metal–aqua and –amine complexes bearing a dioxolene ligand aiming at oxidation of hydrocarbons by the corresponding metal–oxo and –imido complexes.

VIII-A-1 Structural Characterization of Ruthenium–Dioxolene Complexes with Ru^{II}–SQ and Ru^{II}–Cat Frameworks

FUJIHARA, Tetsuaki; OKAMURA, Rei; TANAKA, Koji

[*Chem. Lett.* **34**, 1562–1563 (2005)]

The structural and electronic properties of $[Ru^{II}(trpy)(ClSQ)(PPh_3)]^+$ (trpy = 2,2':6',2''-terpyridine; ClSQ = 4-chlorobenzosemiquinonate) that is prepared from *cis*-$[Ru(trpy)(PPh_3)Cl_2]$ and 4-chlorocatechol (HClCat), and $[Ru^{II}(trpy)(ClCat)(PPh_3)]$ obtained by the reduction of the former were examined. Both complexes were characterized by x-ray diffractometry, UV-visible spectroscopy, ESR, and electrochemistry.

VIII-A-2 Reversible Bond Formation and Cleavage of the Oxo Bridge of $[Ru_2(\mu\text{-}O)(dioxolene)_2(btpyxa)]^{3+}$ [btpyxa = 2,7-Di-tert-butyl-9,9-dimethyl-4,5-bis(2,2':6',2''-terpyrid-4'-yl)xanthene] Driven by a Three-Electron Redox Reaction

WADA, Tohru; TANAKA, Koji

[*Eur. J. Inorg. Chem.* **19**, 3832–3839 (2005)]

The bis(chlororuthenium) complex $[Ru_2Cl_2(3,6\text{-}t\mathrm{Bu}_2\mathrm{sq})_2(btpyxa)](PF_6)_2$ [3,6-*t*Bu_2sq = 3,6-di-*tert*-butyl-1,2-benzosemiquinone; btpyxa = 2,7-di-*tert*-butyl-9,9-dimethyl- 4,5-bis(2,2':6',2''-terpyrid-4'-yl)xanthene] and the oxobridged diruthenium complex $[Ru_2(\mu\text{-}O)(3,6\text{-}t\mathrm{Bu}_2\mathrm{sq})_2(btpyxa)](PF_6)_3$ were synthesized, and the redox behavior of these complexes, which contain a non-innocent dioxolene ligand, was investigated by electrochemistry and electrospectrochemistry methods. Dicationic $\mathbf{2}^+$ undergoes two successive metal-centered one-electron and a simultaneous two-electron ligand-based redox reaction at $E_{1/2}$ = +0.13 and +0.09 and $E_{1/2}$ = –0.75 V (*vs.* SCE), respectively, in CH_2Cl_2. The UV/Vis/NIR spectrum of tricationic $\mathbf{3}^+$ shows an intervalence-transition (IT) band at 1333 nm ($\lambda = 1.52 \times 10^4$ M^{-1} cm^{-1}) in a near-IR region together with two CT bands at 766 ($\lambda = 2.21 \times 10^4$ M^{-1} cm^{-1}) and 586 nm (epsilon = 1.13×10^4 M^{-1} cm^{-1}) in CH_2Cl_2. The mixed-valence complex of $\mathbf{3}^+$ with an Ru^{IV}–O–Ru^{III} core is reversibly oxidized and reduced to the Ru^{IV}–Ru^{IV} and Ru^{III}–Ru^{III} oxidation states at $E_{1/2}$ = +0.63 and –0.01 V, respectively, in CH_2Cl_2. On the other hand, three-electron redn. of $(PF_6)_3$ is accompanied by the cleavage of the Ru–O–Ru bond at E_p = +0.02 V to give [{Ru(OMe)(3,5-*t*Bu_2sq)}{$Ru(OH_2)$(3,5-*t*Bu_2sq)}(btpyxa)]$^+$ in MeOH.

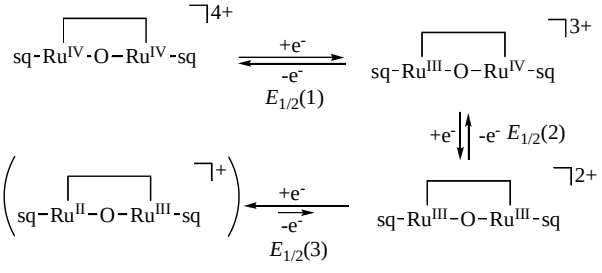

VIII-A-3 A New Series of Molybdenum-(IV), -(V), and -(VI) Dithiolate Compounds as Active Site Models of Molybdoenzymes: Preparation, Crystal Structures, Spectroscopic/ Electrochemical Properties and Reactivity in Oxygen Atom Transfer

SUGIMOTO, Hideki[1]; TARUMIZU, Makoto[1]; TANAKA, Koji; MIYAKE, Hiroyuki[1]; TSUKUBE, Hiroshi[1]
([1]Osaka City Univ.)

[*Dalton Trans.* **21**, 3558–3565 (2005)]

A new set of Mo-(IV), -(V), and -(VI) compounds containing 3,6-dichloro-1,2-benzenedithiolate ($bdtCl_2$) were isolated and characterized by crystallography and other spectroscopic techniques as active site models of arsenite oxidase, one of the molybdoenzymes. MoO_2 compounds were prepared in high yields by reaction of MoO_2Cl_2 with $bdtCl_2$, related dithiolene and thiocatecholate in MeOH at low temp. The $bdtCl_2$ ligand particularly stabilized the MoO compounds with oxidation states of +4 and +5 as well as the MoO_2 compound with an oxidation number of +6. $(Et_4N)_2[Mo^{VI}O_2(bdtCl_2)_2]$ (**1**) $(Et_4N)_2[Mo^{IV}O(bdtCl_2)_2]$ (**2**) and $(Et_4N)[Mo^{V}O(bdtCl_2)_2]$ (**3**) were successfully isolated, whereas $(Et_3NH)_2[MoO_2(thiocatecholate)_2]$ (**6**) gradually decomposed in MeCN. A distorted octahedral structure similar to that of **1** was suggested for the structure of the active site of the oxidized form of arsenite oxidase from a comparison of their bond distances and angles. The bond distances and angles around the Mo(IV) atom in **2** were similar to those around the Mo(IV) center in the reduced form of arsenite oxidase. The reversible 2/3 couple exhibited a more positive redox potential than common MoO dithiolene compounds. **1** underwent an irreversible proton-coupled reduction process to yield **2**. An O atom transfer reaction of **1** with PPh_3 afforded **2** and $OPPh_3$, and proceeded in second order as $v = -d/dt[MoO_2] = k[MoO_2][PPh_3]$. The structures and properties of the oxo-bridged dinuclear compound, $(Et_4N)_2[Mo^{VI}O_2(bdtCl_2)]_2(\mu\text{-}O)$ (**4**), a dimer of $bdtCl_2$ (**5**) and **6** were also characterized.

VIII-A-4 Reversible Hydride Generation and Release from the Ligand of $[Ru(pbn)(bpy)_2](PF_6)_2$ Driven by a Pbn-Localized Redox Reaction

KOIZUMI, Take-aki; TANAKA, Koji

[*Angew. Chem., Int. Ed.* **44**, 5891–5894 (2005)]

$[Ru(pbn)(bpy)_2](PF_6)_2$ (**1**, pbn = 2-(2-pyridyl)benzo[b]-1,5-naphthyridine, bpy = 2,2'-bipyridine) was prepared and characterized by x-ray crystallography. Electrochemical reduction of **1** in an acidic solvent gives $[Ru(pbnH_2)(bpy)_2]^{2+}$ (**2**), which releases the hydrogen as hydride. This catalytic system reduces substrates (for example, acetone) with two electrons and protons from water, and thus operates in a similar way to the NAD^+/NADH redox couple.

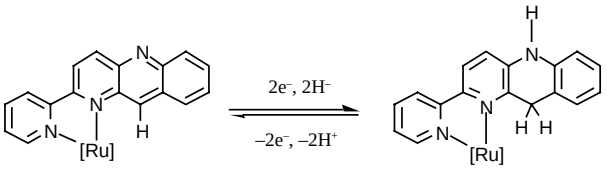

[Ru] = $[Ru(bpy)_2]$

VIII-A-5 Mononuclear Five-Coordinate Molybdenum(IV) and -(V) Monosulfide Complexes Coordinated with Dithiolene Ligands: Reversible Redox of Mo(V)/Mo(IV) and Irreversible Dimerization of $[Mo^{V}S]^-$ Cores to a Dinuclear $[Mo^{V}_2(\mu\text{-}S)_2]^{2-}$ Core

SUGIMOTO, Hideki[1]; SAKURAI, Takashi[1]; MIYAKE, Hiroyuki[1]; TANAKA, Koji; TSUKUBE, Hiroshi[1]
([1]Osaka City Univ.)

[*Inorg. Chem.* **44**, 6927–6929 (2005)]

A mononuclear five-coordinate Mo(IV) monosulfide complex, $(Et_4N)_2[MoS(L)_2]$ (L = cyclohexene-1,2-dithiolate) (**1**), was obtained and characterized by IR, UV-visible spectroscopic methods, and x-ray crystallography. **1** was oxidized by an equiv. ferrocenium cation to give the corresponding mononuclear Mo(V) complex, $(Et_4N)[MoS(L)_2]$ (**2**), which was stable for a few minutes under a lower concentration than 0.3 mM and then further dimerized to $(Et_4N)_2[Mo(L)_2]_2(\mu\text{-}S)_2$ (**3**).

VIII-A-6 Synthesis and Crystal Structures of $[W(3,6\text{-dichloro-1,2-benzenedithiolate})_3]^{n-}$ (n = 1, 2) and $[Mo(3,6\text{-dichloro-1,2-benzenedithiolate})_3]^{2-}$: Dependence of the Coordination Geometry on the Oxidation Number and Counter-Cation in Trigonal-Prismatic and Octahedral Structures

SUGIMOTO, Hideki[1]; FURUKAWA, Yuuki[1]; TARUMIZU, Makoto[1]; MIYAKE, Hiroyuki[1]; TANAKA, Koji; TSUKUBE, Hiroshi[1]
([1]Osaka City Univ.)

[*Eur. J. Inorg. Chem.* **15**, 3088–3092 (2005)]

$(Et_4N)_2[W(bdtCl_2)_3]$ (**1a**), $(Ph_4P)_2[W(bdtCl_2)_3]$ (**1b**), $(Et_4N)[W(bdtCl_2)_3]$ (**2a**), $(Ph_4P)[W(bdtCl_2)_3]$ (**2b**), $(C_5NH_6)[W(bdtCl_2)_3]$ (**2c**), and $(Et_3NH)_2[Mo(bdtCl_2)_3]$ (**3a**) ($bdtCl_2$ = 3,6-dichloro-1,2-benzenedithiolate) were prepared and characterized by x-ray crystallography, UV/visible spectroscopic, and electrochemical methods. Versatile geometrical changes around the W centers were observed. The trigonal-prismatic structure of the W center in $(Et_4N)_2[W(bdtCl_2)_3]$ (**1a**) is changed to an intermediate structure between trigonal prismatic and octahedral upon solid-state oxidation of the complex of **2a**. Replacement of the countercation of **1a** with Ph_4P^+ also resulted in geometrical changes and somewhat of an octahedral contribution is included in **1b**. However, almost the same coordination structures are present in structures **2a**, **2b**, and **2c**, with an oxidation number of

+5. These structures adopt an intermediate geometry between trigonal prismatic and octahedral. No geometrical change was observed upon changing the metal center from W to Mo in $[M(bdtCl_2)_3]^{2-}$ (M = W and Mo).

VIII-A-7 Synthesis, Structures and Electrochemical Properties of Ruthenium (II) Complexes Bearing Bidentate 1,8-Naphthyridine and Terpyridine Analogous (N,N,C)-Tridentate Ligands

KOIZUMI, Take-aki; TOMON, Takashi; TANAKA, Koji

[*J. Organomet. Chem.* **690**, 4272–4279 (2005)]

1,8-Naphthyridine (napy) and terpyridine-analogous (N,N,C) tridentate ligands coordinated ruthenium (II) complexes, $[RuL(napy\text{-}kappa2,N,N')(dmso)](PF_6)_2$ (**1**: L = L1 = N''-methyl-4'-methylthio-2,2':6',4''-terpyridinium, **2**: L = L2 = N''-methyl-4'-methylthio-2,2':6',3''-terpyridinium) were prepared and their chemical and electrochemical properties were characterized. The structure of complex **1** was determined by x-ray crystallographical study, showing that it has a distorted octahedral coordination style. The cyclic voltammogram of **1** in DMF exhibited two reversible ligand-localized redox couples. On the other hand, the CV of **2** shows two irreversible cathodic peaks, due to the Ru–C bond of **2** containing the carbenic character. The IR spectra of 1 in CO_2-saturated CH_3CN showed the formation of Ru–(η–CO_2) and Ru–CO complexes under the controlled potential electrolysis of the solution at –1.44 V (*vs*. Fc/Fc^+). The electrochemical reduction of CO_2 catalyzed by **1** at –1.54 V (*vs*. Fc/Fc^+) in DMF (–0.1 M Me_4NBF_4) produced CO with a small amt. of HCO_2H.

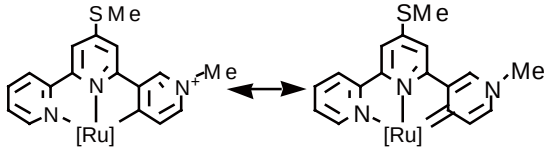

VIII-A-8 Dioxo-Molybdenum(VI) and Mono-Oxo-Molybdenum(IV) Complexes Supported by New Aliphatic Dithiolene Ligands: New Models with Weakened Mo:O Bond Characters for the Arsenite Oxidase Active Site

SUGIMOTO, Hideki[1]; HARIHARA, Makoto[1]; SHIRO, Motoo[1]; SUGIMOTO, Kunihisa[1]; TANAKA, Koji; MIYAKE, Hiroyuki[1]; TSUKUBE, Hiroshi[1]
([1]Osaka City Univ.)

[*Inorg. Chem.* **44**, 6386–6392 (2005)]

The *cis*-dioxomolybdenum(VI) complexes, $[MoO_2(LH)_2]^{2-}$ (**1b**), $[MoO_2(LS)_2]^{2-}$ (**2b**), and $[MoO_2(LO)_2]^{2-}$ (**3b**) (LH = cyclohexene-1,2-dithiolate, LS = 2,3-dihydro-2H-thiopyran-4,5-dithiolate, and LO = 2,3-dihydro-2H-pyran-4,5-dithiolate), with new aliphatic dithiolene ligands were prepared and studied by IR and UV-visible spectroscopic and electrochemical methods. The mono-oxomolybdenum(IV) complexes, $[MoO(LH)_2]^{2-}$ (**1a**), $[MoO(LS)_2]^{2-}$ (**2a**), and $[MoO(LO)_2]^{2-}$ (**3a**), were further characterized by x-ray crystal structural determinations. The IR and resonance Raman spectroscopic studies suggested that these *cis*-dioxo Mo(VI) complexes (**1b**-**3b**) have weaker Mo=O bonds than the common $Mo^{VI}O_2$ complexes. Complexes **1b**-**3b** also exhibited strong absorption bands in the visible regions assigned as charge-transfer bands from the dithiolene ligands to the *cis*-MoO_2 cores. Because the O atoms of the *cis*-$Mo^{VI}O_2$ cores are relatively nucleophilic, these complexes are unstable in protic solvents and protonation might occur to produce $Mo^{VI}O(OH)$, as observed with the oxidized state of arsenite oxidase.

VIII-A-9 Electronic Structural Changes between Nickel(II)–Semiquinonato and Nickel(III)–Catecholato States Driven by Chemical and Physical Perturbation

OHTSU, Hideki; TANAKA, Koji

[*Eur. J. Chem. A* **11**, 3420–3426 (2005)]

The selective synthesis of tetracoordinate square-planar low-spin nickel(II)–semiquinonato (Ni^{II}–SQ) and nickel(III)–catecholato (Ni^{III}–Cat) complexes, [Ni(L)(SQ/CAT)](PF_6) (L = dibenzyl(2-pyridylmethyl)amine, SQ = 3,5-di-*tert*-butylsemiquinonate, CAT = 3,5-di-*tert*-butylcatecholate), **1** and **2**, respectively, was achieved by using bidentate ligands with modulated nitrogen-donor ability to the nickel ion. The electronic structures of **1** and **2** were revealed by XPS and EPR measurements. The absorption spectra of **1** and **2** in a noncoordinating solvent, dichloromethane (CH_2Cl_2), are completely different from those in THF, being a coordinating solvent. As expected the gradual addition of DMF, which is also a coordinating solvent like THF, into a solution of **1** or **2** in CH_2Cl_2 leads to color changes from blue (for **1**) and brown (for **2**) to light green, which is the same color observed for solutions of **1** or **2** in THF. Also, the same color changes are induced by varying the temp. Such spectral changes are attributable to the transformation from square-planar low-spin Ni^{II}–SQ and Ni^{III}–Cat complexes to octahedral high-spin Ni^{II}–SQ ones, caused by the coordination of two solvent molecules to the nickel ion.

VIII-A-10 Electrochemical Hydrogenation of $[Ru(bpy)_2(napy\text{-}\kappa N)(CO)]^{2+}$: Inhibition of Reductive Ru–CO Bond Cleavage by a Ruthenacycle

TOMON, Takashi; KOIZUMI, Take-aki; TANAKA, Koji

[*Angew. Chem., Int. Ed.* **44**, 2229–2232 (2005)]

A 5-membered metallacycle ($\mathbf{2}^+$) hydrogenated at the 4-position of the naphthyridine ligand ($\mathbf{3}^+$) is formed by the electrochemical reduction of $[Ru(bpy)_2(napy\text{-}\kappa N)(CO)]^{2+}$ ($\mathbf{1}^{2+}$; bpy = 2,2'-bipyridine, napy = 1,8-naphthyridine) at –1.40 V in H_2O. Chemical or electro-

chemical oxidation of $\mathbf{3}^+$ regenerates $\mathbf{1}^+$ through $\mathbf{2}^+$ in almost quantitative yield.

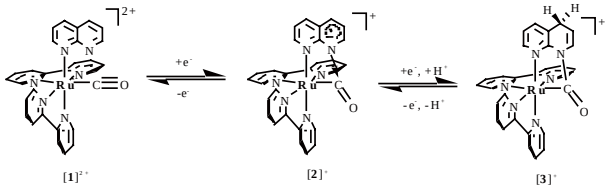

VIII-A-11 Synthesis, Chemical- and Electrochemical Properties of Ruthenium(II) Complexes Bearing 2,6-Bis(2-naphthyridyl)pyridine

KOIZUMI, Take-aki; TANAKA, Koji

[*Inorg. Chim. Acta* **358**, 1999–2004 (2005)]

Ruthenium complexes with a terpyridine-analogous ligand, 2,6-bis(2-naphthyridyl)- pyridine (**I**, bnp), were synthesized and their chemical and electrochemical properties studied. The structures of $[Ru(bnp)(tpy)](PF_6)_2$ (**1**) and $[Ru(bnp)_2](PF_6)_2$ (**2**) were determined by x-ray structure analysis. The bnp localized redox potentials of **1** and **2** showed significant positive shift by 260–290 mV relative to the analogous Ru–terpyridine complexes.

VIII-A-12 Synthesis and Electrochemical Properties of Bis(bipyridine)ruthenium(II) Complexes Bearing Pyridinyl- and Pyridinylidene Ligands Induced by Cyclometalation of N-Methylated Bipyridinium Analogs

KOIZUMI, Take-aki; TOMON, Takashi; TANAKA, Koji

[*J. Organomet. Chem.* **690**, 1258–1264 (2005)]

Ruthenium cyclometalated complexes with N-monomethylated 2,4'- and 2,3'-bipyridine N,C-ligands were prepared and characterized. Reaction of $[(bpy)_2RuCl_2]$ (bpy = 2,2'-bipyridine) with 1-methyl-4-(2-pyridinyl) pyridinium ($HL_1 \cdot PF_6$) and 1-methyl-3-(2-pyridinyl) pyridinium ($HL_2 \cdot PF_6$) hexafluorophosphates and $AgPF_6$ afforded cyclometalated complexes $[(bpy)_2Ru(L_1\text{-}C3, N')][PF_6]_2$ (**1**) and carbenoid complex **I** (**2**), respectively. Structure of **2** was confirmed by low-field shift of the C4-carbon of the cyclometalated bipyridinium ligand and by x-ray structure determination. The ligand-localized redox potentials of **1** and **2** also revealed the substantial difference in the electron donating ability of both ligands.

VIII-A-13 Stabilization and Destabilization of the Ru–CO Bond during the 2,2'-Bipyridin-6-Onato (bpyO)-Localized Redox Reaction of $[Ru(terpy)(bpyO)(CO)](PF_6)$

TOMON, Takashi; KOIZUMI, Take-aki; TANAKA, Koji

[*Eur. J. Inorg. Chem.* **2**, 285–293 (2005)]

Two stereoisomers of $[Ru(terpy)(bpyO)(CO)](PF_6)$ ($[\mathbf{1}]^+$ and $[\mathbf{2}]^+$; terpy = 2,2':6',2''-terpyridine, bpyO = 2,2'-bipyridin-6-onato) were prepared. The pyridonato moiety in the bpyO ligand of $[\mathbf{1}]^+$ and $[\mathbf{2}]^+$ is located *trans* and *cis*, respectively, to CO. Treatment of $[\mathbf{1}]^+$ and $[\mathbf{2}]^+$ with HPF_6 produced $[\mathbf{1}H]^{2+}$ and $[\mathbf{2}H]^{2+}$, both of which contain bpyOH (bpyOH = 6-hydroxy-2,2'-bipyridine). The difference in the *pKa* values of $[\mathbf{1}H]^{2+}$ (3.5) and $[\mathbf{2}H]^{2+}$ (3.9) reflects the stronger electronic interaction between CO and the pyridonato moiety in the bpyO ligand in the *trans* position compared with that in the *cis* position. The molecular structures of $[\mathbf{1}](PF_6)$, $[\mathbf{2}](PF_6)\cdot H_2O$ and $[\mathbf{2}H](PF_6)_2\cdot 2H_2O$ were determined by x-ray structure analyses. $[\mathbf{1}]^+$ and $[\mathbf{2}]^+$ undergo one reversible reduction at $E_{1/2}$ = –1.65 V and –1.51 V, respectively, and one irreversible reduction at $E_{p,c}$ = –2.07 and $E_{p,c}$ = –2.13 V, respectively. Both reductions are assigned to redox reactions localized at the terpy and bpyO ligands. Irreversible reduction of $[\mathbf{1}]^0$ results from reductive cleavage of the Ru–CO bond of $[\mathbf{1}]^-$. However, a two-electron oxidation of $[\mathbf{2}]^-$ almost regenerates $[\mathbf{2}]^+$ because of the depression of the reductive Ru–CO bond cleavage of $[\mathbf{2}]^-$ due to cyclometalation formed by an attack of O of bpyO to the C of the Ru–CO bond. An unusually large shift of the ν(C≡O) band on going from $[\mathbf{2}]^0$ (1950 cm^{-1}) to $[\mathbf{2}]^-$ (1587 cm^{-1}) also supports a reversible cyclometalation driven by the bpyO-localized redox reaction.

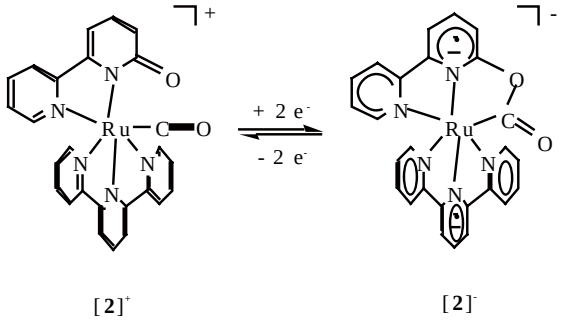

VIII-A-14 Electronic Structural Changes between Nickel(II)–Semiquinonato and Nickel(III)–Catecholato States Driven by Chemical and Physical Perturbation

OHTSU, Hideki; TANAKA, Koji

[*Eur. J. Chem. A* **11**, 3420–3426 (2005)]

The selective synthesis of tetracoordinate square-planar low-spin nickel(II)–semiquinonato (Ni^{II}–SQ) and nickel(III)–catecholato (Ni^{III}–Cat) complexes, [Ni(L)(SQ/CAT)](PF_6) (L = dibenzyl(2-pyridylmethyl)amine, SQ = 3,5-di-*tert*-butylsemiquinonate, CAT = 3,5-di-*tert*-butylcatecholate), **1** and **2**, respectively, was achieved by using bidentate ligands with modulated nitrogen-donor ability to the nickel ion. The electronic structures of **1** and **2** were revealed by XPS and EPR measurements. The absorption spectra of **1** and **2** in a noncoordinating solvent, dichloromethane (CH_2Cl_2), are completely different from those in THF, being a coordinating sol-

vent. As expected the gradual addition of DMF, which is also a coordinating solvent like THF, into a solution of **1** or **2** in CH_2Cl_2 leads to color changes from blue (for **1**) and brown (for **2**) to light green, which is the same color observed for solutions of **1** or **2** in THF. Also, the same color changes are induced by varying the temp. Such spectral changes are attributable to the transformation from square-planar low-spin Ni^{II}–SQ and Ni^{III}–Cat complexes to octahedral high-spin Ni^{II}–SQ ones, caused by the coordination of two solvent molecules to the nickel ion.

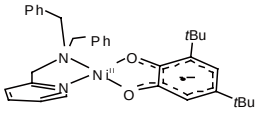

$[Ni^{II}(Py(Bz)_2)(tBu_2SQ)](PF_6)$

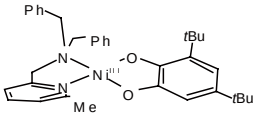

$[Ni^{III}(MePy(Bz)_2)(tBu_2Cat)](PF_6)$

VIII-B Coordination Chemistry of Sterically Hindered Ligands and Multidentate Ligands, and Activation of Small Molecules

This project is focused on the design and synthesis of new ligands that are capable of supporting novel structural features and reactivity. Currently, we are investigating multidentate ligands based on aryloxide and thiolate. In addition, we set out to study metal complexes with sterically hindered aryloxide and arylthiolate ligands. Our recent efforts have been directed toward activation of small molecules.

VIII-B-1 Complexes of Tantalum with Triaryloxides: Ligand and Solvent Effects on Formation of Hydride Derivatives

KAWAGUCHI, Hiroyuki; MATSUO, Tsukasa

[*J. Organomet. Chem.* **690**, 5333–5345 (2005)]

A family of tantalum compounds supported by the triaryloxide $[R–L]^{3–}$ ligands are reported [H_3(R–L) = 2,6-bis(4-methyl-6-R-salicyl)-4-*tert*-butylphenol, where R = Me or Bu^t]. The reaction of H_3[Me–L] with $TaCl_5$ in toluene gave $[(Me–L)TaCl_2]_2$ (**1**). The [Bu^t–L] analogue $[(Bu^t–L)TaCl_2]_2$ (**2**) was synthesized *via* treatment of $TaCl_5$ with $Li_3[Bu^t–L]$. A THF solution of $LiBHEt_3$ was added to **1** in toluene to provide $[(Me–L)TaCl(THF)]_2$ (**3**), while treatment of **2** with 2 equiv of $LiBHEt_3$ or potassium in toluene followed by recrystallization from DME resulted in formation of $[M(DME)_3][\{(Bu^t–L)TaCl\}_2(\mu\text{-}Cl)]$ [M = Li (**4a**), K (**4b**)]. When the amount of $MBHEt_3$ (M = Li, Na, K) was increased to 5 equiv, the analogous reactions in toluene afforded $[\{(bit\text{-}Bu^t–L)Ta\}_2(\mu\text{-}H)_3M]$ [M = $Li(THF)_2$ (**5a**), $Na(DME)_2$ (**5b**), $K(DME)_2$ (**5c**)]. During the course of the reaction, the methylene CH activation of the ligand took place. Dissolution of **5a** in DME produced $[\{(bit\text{-}Bu^t–L)Ta\}_2(\mu\text{-}H)_3Li(DME)_2]$ (**6**), indicating that the coordinated THF molecules are labile. When the **2**/$LiBHEt_3$ reaction was carried out in THF, the ring opening of THF occurred to yield $[(Bu^t–L)Ta(OBu^n)_2]_2$ (**7**) along with a trace amount of $[Li(THF)_4][\{(Bu^t–L)TaCl\}_2(\mu\text{-}OBu^n)]$ (**8**). Treatment of **2** with potassium hydride in DME yielded $[\{(Bu^t–L)TaCl_2K(DME)_2\}_2(\mu\text{-}OCH_2CH_2O)]$ (**9**), in which the ethane-1,2-diolate ligand arose from partial C–O bond rupture of DME.

VIII-B-2 A Synthetic Cycle for H_2/CO Activation and Allene Synthesis Using Recyclable Zirconium Complexes

MATSUO, Tsukasa; KAWAGUCHI, Hiroyuki

[*J. Am. Chem. Soc.* **127**, 17198–17199 (2005)]

Fischer–Tropsch (F–T) synthesis is an important chemical reaction to convert H_2 and CO to hydrocarbons along with water, thereby giving access to organic chemistry on the basis of simple inorganic molecules. The impressive F–T chemical transformation has elicited extensive synthetic efforts to reach chemical understanding of the heterogeneous F–T reaction and to produce soluble metal complexes that can react with H_2 and CO to form hydrocarbons with high product selectivity. Although many soluble metal compounds and reactions relevant to surface species in the heterogeneous F–T process are known, well-characterized synthetic systems capable of converting H_2/CO into hydrocarbons have been limited. To explore the transformation of H_2 and CO with metal complexes, we have sought to use zirconium complexes supported by 2,6-bis(3-*tert*-butyl-5-methyl-2-oxybenzyl)-4-R-anisole ligands ($[L^R]^{2–}$).

This study demonstrated a synthetic cycle having relevance to F–T chemistry, wherein zirconium alkyl complexes of the $[L^R]$ ligands serves to transform H_2 and CO into corresponding allenes *via* alkylidene intermediates. The synthetic cycle is outlined in Scheme 1. This transformation involves the activation of H_2, and C–C, C–H bond formation, C–O bond cleavage, and deoxygenative recycling of the oxo-bridging zirconium complexes. All of the preceding reactions are spectroscopically quantitative under mild conditions. Thus there is much potential for yield optimization, including the combination of consecutive steps.

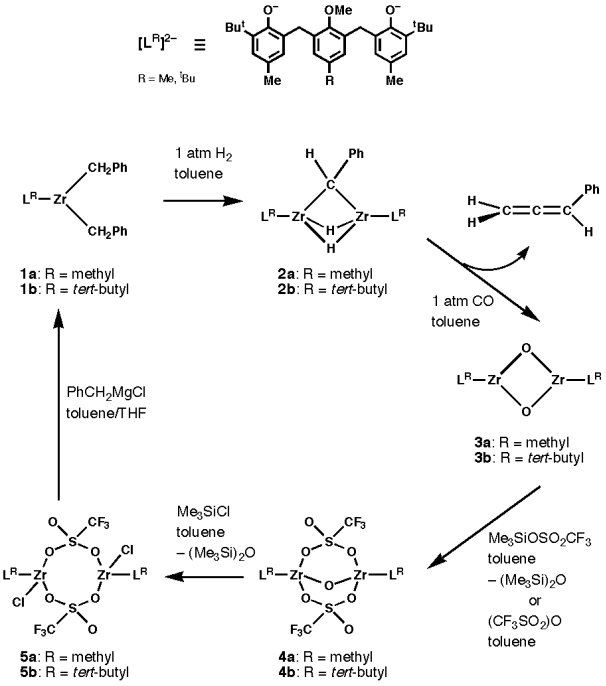

Scheme 1.

VIII-B-3 A Tantalum(V) Carbene Complex: Formation of a Carbene-Bis(phenoxide) Ligand by Sequential Proton and Hydride Abstraction

WATANABE, Takahito; MATSUO, Tsukasa; KAWAGUCHI, Hiroyuki

[*Inorg. Chem.* **45**, 6580–6582 (2006)]

Bis(phenoxides), in which the two phenoxide rings are linked to a donor atom (X) such as sulfur and phosphorous in the *ortho* positions, have been useful dianionic ancillary ligands in coordination chemistry and homogeneous catalysis. In this type of [**OXO**] ligands that combine the hard phenoxide donors with the soft X donor into a chelating array, electronic and stereochemical parameters can be manipulated by modifications of X donor groups so as to accommodate many transition metals in a variety of oxidation states and induce interesting transformations. With this in mind, we have begun to study the chemistry of carbene–phenoxide hybrid ligands, where a carbene functionality is introduced at the X donor site. The strong two-electron donor ability of the carbene group was appealing to us. In addition, this ligand system would provide the opportunity to study the effect of the σ-donor carbene functionality on the properties of electron deficient metal complexes.

The present work has demonstrated the synthesis and structure of the cationic tantalum(V) dimethyl complex with the [**OCO**] ligand. The dianionic tridentate [**OCO**] ligand is formed by the sequential proton and hydride abstraction from the backbone of the [**OO**] ligand (Scheme 1). The carbene moiety of **3** is stabilized *via* π-bonding to the oxyphenyl groups. This kind of carbene in this circumstance could be viewed as a neutral σ-donor carbene bound to Ta(V). This is a rare example of early transition metal complexes with σ-donor carbene ligands except N-heterocyclic carbenes. The electrophilic nature of carbene **3** has been shown in the reaction with PPh_3. Extension of this work to include other transition metal complexes and reactivity studies of **3** are in progress.

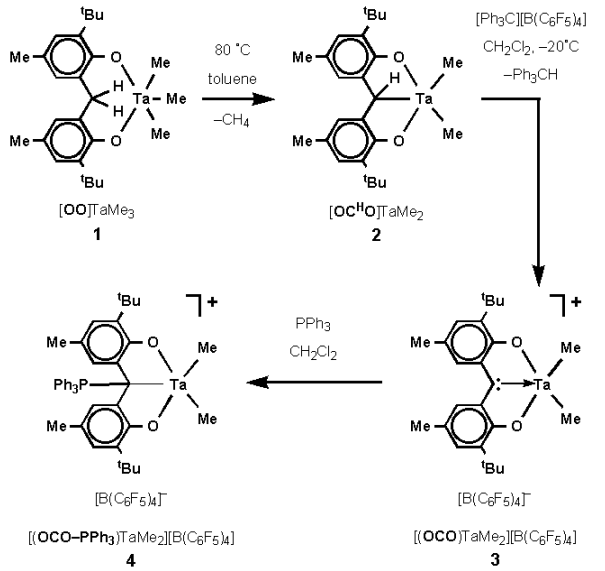

Scheme 1.

VIII-C Physicochemical Properties of Hemoprotein Reconstituted with Artificially Created Hemins

Hemoprotein is one of the most versatile metalloproteins having a prosthetic group heme, *e.g.* protoheme IX, which shows various physicochemical properties. Most of hemes in hemoproteins are usually bound in the heme pocket via multiple non-covalent interactions with the several amino acid residues. Recently, we have focused on the replacement of the native hemin with an artificially created metal complex. This method is at least two advantages; First, the reconstitution with an artificial hemin gives an insight into the elucidation of hemoprotein function. Second, we have a chance to dramatically modify the function of hemoproteins. In our project, we try to prepare various artificial prosthetic groups and inserted them into apohemoproteins to obtain reconstituted proteins. For example, one of our aims is to elucidate the role of each heme-propionate side chains in a series of hemoproteins by replacing the native hemin with monopropionated hemin. Replacing the native hemin with hemin derivatives such as iron porphycene or iron corrole is also very attractive to modify the function of hemoproteins. From these projects, we wish to understand the physicochemical properties of hemoproteins based on the coordination chemistry in the protein matrix.

VIII-C-1 Preparation and O_2 Binding Study of Myoglobin Having a Cobalt Porphycene

MATSUO, Takashi[1]; TSURUTA, Takashi[2]; MAEHARA, Keiko[2]; SATO, Hideaki[2]; HISAEDA, Yoshio[2]; HAYASHI, Takashi[3]
([1]Osaka Univ.; [2]Kyushu Univ.; [3]IMS and Osaka Univ.)

[*Inorg. Chem.* **44**, 9391–9396 (2005)]

Sperm whale myoglobin, an oxygen-storage hemoprotein, was reconstituted with 2,7-diethyl-3,6,12,17-tetramethyl-13,16-bis(carboxyethyl)porphycenatocobalt (II) in order to investigate the reactivities of a cobalt porphycene in a protein matrix (Figure 1). Similar to the previously reported finding for the myoglobin with the iron porphycene, the reconstituted myoglobin with the cobalt porphycene was also found to have a higher O_2 affinity by two orders of magnitude when compared to the myoglobin possessing cobalt protoporphyrin IX. The EPR spectra of the deoxy and oxy myoglobins having the cobalt porphycene at 77 K also have similar features to the myoglobin with cobalt protoporphyrin IX. These spectra suggest that the porphycene cobalt in the deoxy form is coordinated by one nitrogenous ligand postulated to be the imidazole ring of His93, and that the bond configuration of Co^{II}–O_2 is regarded as the Co^{III}–$O_2^{\bullet-}$ species.

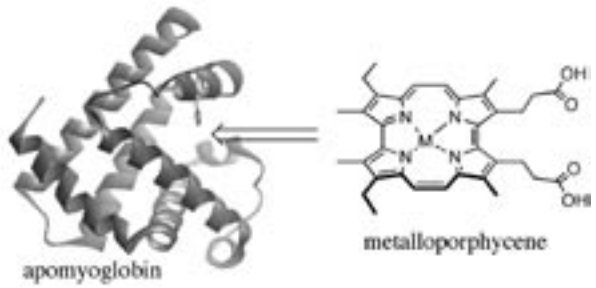

Figure 1. Incorporation of metalloporphycene into apomyoglobin.

VIII-C-2 Iron Porphyrin–Cyclodextrin Supramolecular Complex as a Functional Model of Myoglobin in Aqueous Solution

KANO, Koji[1]; KITAGISHI, Hiroaki[1]; DAGALLIER, Camelle[1]; KODERA, Masahito[1]; MATSUO, Takashi[2]; HAYASHI, Takashi[3]; HISAEDA, Yoshio[4]; HIROTA, Shun[5]
([1]Doshisha Univ.; [2]Osaka Univ.; [3]IMS and Osaka Univ.; [4]Kyushu Univ.; [5]Kyoto Pharm. Univ.)

[*Inorg. Chem.* **45**, 4448–4460 (2006)]

The 1:1 inclusion complex of 5,10,15,20-tetrakis(4-sulfonatophenyl)porphinatoiron(II) (Fe^{II}TPPS) and an *O*-methylated β-cyclodextrin dimer having a pyridine linker (**1**) binds dioxygen reversibly in aqueous solution. The O_2 adduct was very stable ($t_{1/2}$ = 30.1 h) at pH 7.0 and 25 °C. ESI-MS and NMR spectroscopic measurements and molecular mechanics calculations indicated the inclusion of the sulfonatophenyl groups at the 5- and 15-positions of Fe^{III}TPPS or Fe^{II}TPPS into two cyclodextrin moieties of **1** to form a supramolecular 1:1 complex (hemoCD1 for the Fe^{II}TPPS complex), whose iron center is completely covered by two cyclodextrin moieties. Equilibrium measurements and laser flash photolysis provided the affinities ($P^{O2}{}_{1/2}$ and $P^{CO}{}_{1/2}$) and rate constants for O_2 and CO binding of hemoCD1 ($k^{O2}{}_{on}$, $k^{O2}{}_{off}$, $k^{CO}{}_{on}$, and $k^{CO}{}_{off}$). The CO affinity relative to the O_2 affinity of hemoCD1 was abnormally high. Although resonance Raman spectra suggested weak back-bonding of $d\pi(Fe) \rightarrow \pi^*(CO)$ and hence a weak CO–Fe bond, the CO adduct of hemoCD1 was very stable. The hydrophobic CO molecule dissociated from CO-hemoCD1 hardly breaks free from a shallow cleft in hemoCD1 surreounded by an aqueous bulk phase leading to fast rebinding of CO to hemoCD1. Isothermal titration calorimetry furnished the association constant (K^{O2}), $\Delta H°$, and $\Delta S°$ for O_2 association to be (2.71±0.51) × 10^4 M^{-1}, –65.2±4.4 kJ mol^{-1}, and –133.9 ±16.1 J mol^{-1} K^{-1}, respectively. The autoxidation of oxy-hemo CD1 was accelerated by H^+ and OH^-. The inorganic anions also accelerated the autoxidation of oxy-hemo CD1. The O_2–Fe^{II} bond is equivalent to the $O_2^{\bullet-}$–Fe^{III} bond, which is attacked by the inorganic anions or the

water molecule to produce met–hemoCD1 and a superoxide anion.

VIII-C-3 Crystal Structure and Peroxidase Activity of Myoglobin Reconstituted with Iron Porphycene

HAYASHI, Takashi[1]; MURATA, Dai[2]; MAKINO, Masatomo[3]; SUGIMOTO, Hiroshi[4]; MATSUO, Takashi[5]; SATO, Hideaki[2]; SHIRO, Yoshitsugu[4]; HISAEDA, Yoshio[2]
([1]IMS and Osaka Univ.; [2]Kyushu Univ.; [3]Himeji Inst. Tech.; [4]RIKEN/SPring-8; [5]Osaka Univ.)

[*Inorg. Chem.* to be submitted]

The incorporation of an artificially created metal complex into an apomyoglobin is one of the attractive studies in a series of hemoprotein modifications. Single crystals of myoglobin reconstituted with 13,16-dicarboxyethyl-2,7-diethyl-3,6,12,17-tetramethylporphycenatoiron(III) were obtained in the imidazole buffer and the 3D structure with a 2.25-Å resolution indicates that the artificially created prosthetic group as a heme structural isomer is located in the normal position of the heme pocket (Figure 1). Furthermore, the reconstituted myoglobin catalyzed the H_2O_2-dependent oxidations of substrates such as guaiacol, thioanisole, and styrene. At pH 7.0 and 20 °C, the initial rate of the guaiacol oxidation is 11-fold faster than that observed for the native myoglobin. Moreover, the stopped-flow studies of the reconstituted protein with H_2O_2 demonstrated that two reaction intermediates, compounds II and III, were detected in the absence of a substrate. It is a rare example that compound III is formed via compound II in myoglobin chemistry. The enhancement of the peroxidase activity and the formation of the stable compound III in myoglobin with iron porphycene could be due to the strong coordination of the Fe–His93 bond.

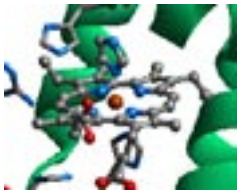

Figure 1. 3D crystal structure of iron(III)-porphycene in myoglobin matrix.

VIII-C-4 Construction of Glycosylated Myoglobin by Reconstitutional Method

MATSUO, Takashi[1]; NAGAI, Hirokazu[2]; HISAEDA, Yoshio[2]; HAYASHI, Takashi[3]
([1]Osaka Univ.; [2]Kyushu Univ.; [3]IMS and Osaka Univ.)

[*Chem. Commun.* **29**, 3131–3133 (2006)]

An artificially created prosthetic group **1** having β-galactosyl moieties (Figure 1) was prepared and inserted into sperm whale apomyoglobin to successfully afford a glycosylated myoglobin. The glycomyoglobin was characterized by ESI-MS and UV-vis spectroscopy and stable in a buffer solution at 4 °C over one week. The immunoprecipitaton experiment was carried out to evaluate the function of the galactose units on the protein surface. The mixture of the glycomyoglobin and commercially available biotin-labelled peanut lectin was treated with streptavidin-modified sepharose to determine the affinity. From this study, the galactose units on the myoglobin surface well work as the interface for forming the myoglobin–lectin complex without any non-specific interaction.

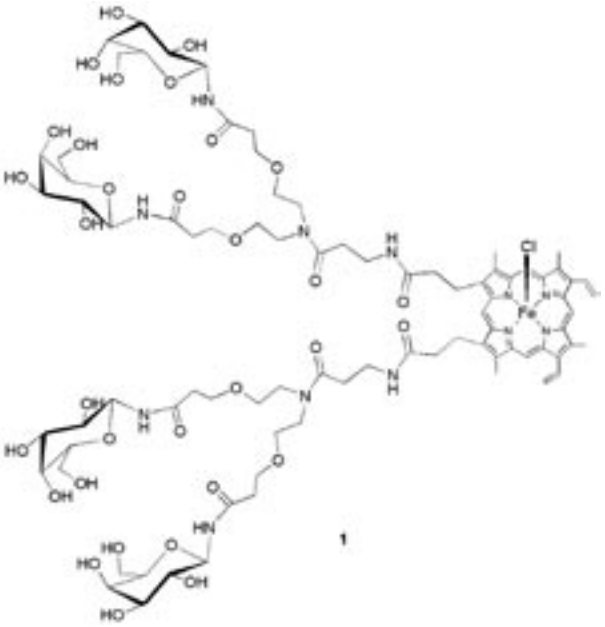

Figure 1. Galactohemin **1** as an artificial prosthetic group for myoglobin.

VIII-C-5 Structure and Ligand Binding Properties of Sperm Whale Myoglobins Reconstituted with Two Monopropionated Hemin: Role of Each Heme-Propionate Side Chain in Myoglobin

HAYASHI, Takashi[1]; HARADA, Katsuyoshi[2]; MAKINO, Masatomo[3]; HIROTA, Shun[4]; SUGIMOTO, Hiroshi[5]; MATSUO, Takashi[2]; SHIRO, Yoshitsugu[5]; FUNASAKI, Noriaki[4]; HISAEDA, Yoshio[6]
([1]IMS and Osaka Univ.; [2]Osaka Univ.; [3]Himeji Inst. Tech.; [4]Kyoto Pharm. Univ.; [5]RIKEN/SPring-8; [6]Kyushu Univ.)

[*J. Am. Chem. Soc.* to be submitted]

Many hemoproteins have protoheme IX as a prosthetic group. The heme bears two unique propionate side chains at 6- and 7-positions of β-pyrrolic carbons. According to a series of 3D structures of hemoproteins, the propionate side chains interact with polar amino acid residues in the protein matrix, so it has been known that the side chains play a role on the fixation of the prosthetic group in the heme pocket. However, we have recently thought that the role of the two propionate side chains are not only the fixation of heme but also the direct contribution to the regulation of the hemoprotein

function. Based on this viewpoint, we have prepared two monopropionated hemes; 6-methyl-7-carboxyethyl-heme (6M7PHE) and 6-carboxyethyl-7-methyl-heme (6P7MHE) (Figure 1). Furthermore, the hemins were incorporated into apohemoprotein by conventional method to understand each role of the defective propionate side chain.

In the case of sperm whale myoglobin, 6- and 7-propionate side chains interact with Arg45 and Ser92 via hydrogen bonding, respectively. The reconstituted myoglobins with the two monopropionated hemins, rMb (6M7PHE) and rMb(6P7MHE), were characterized by UV-vis, ESI-MS, 1H NMR spectroscopic methods. The dissociation of O_2 from oxymyoglobin with 6M7PHE was accelerated about three times as that of the oxymyoglobin with the native heme. Furthermore, the autoxidation rate of oxymyoglobin with 6M7PHE was approximately six times faster than that of oxymyoglobin with native heme. These results indicate that the 6-propionate side chain plays an important role on the stabilization of oxymyoglobin. In contrast, the acceleration of the CO binding rate was observed for myoglobin with 6P7MHE, suggesting that the 7-propionate side chain regulates the His93–heme iron coordination in the proximal site.

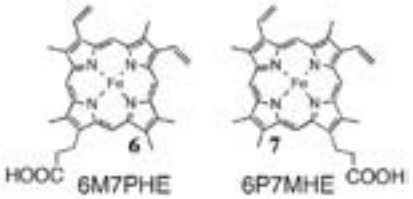

Figure 1. Structures of Two Monopropionated Heme.

VIII-C-6 Ligand Binding Properties of Two Kinds of Reconstituted Myoglobins with Iron Porphycene Having Propionates: Effect of β-Pyrrolic Position of Two Propionate Side Chains in Porphycene Framework

MATSUO, Takashi[1]; IKEGAMI, Takahiro[2]; SATO, Hideaki[2]; HISAEDA, Yoshio[2]; HAYASHI, Takashi[3]
([1]Osaka Univ.; [2]Kyushu Univ.; [3]IMS and Osaka Univ.)

[*J. Inorg. Biochem.* **100**, 1265–1271 (2006)]

An iron porphycene containing two propionate side chains at the 12th and 17th β-pyrrolic positions of the porphycene ring was synthesized and incorporated into sperm whale apomyoglobin in order to investigate the O_2 and CO binding properties of the reconstituted ferrous myoglobin. The protein showed a slower O_2 dissociation rate by 1/20, compared to the native myoglobin, whereas the CO dissociation rates were found to be almost the same. This tendency is similar to the result of a previous study on the reconstituted myoglobin with a porphycene having the propionates at the 13th and 16th b-pyrrolic positions. However, the present myoglobin showed a faster O_2 dissociation than the previously studied myoglobin. This finding suggests that the position of the two propionates as well as the symmetry of the porphycene framework is an important factor for obtaining a stable oxygenated iron porphycene myoglobin.

VIII-D Syntheses, Structures, and Reactivities of Multinuclear Transition Metal Complexes with O- and N-Donor Ligands

Organotransition metal complexes with O- and N-donor ligands have recently been attracting considerable attention, because they often show structures, reactivities, and physicochemical properties significantly different from those of the complexes with P- and S-donor ligands. In this project it has been revealed that cyanamide (NCN^{2-}) anion effectively bridge organometallic fragments to form multinuclear complexes with characteristic structures. It has recently been found that tetranuclear C_3-elongated cubane-like complexes of cobalt and rhodium can be synthesized from the reaction of $[Cp^*MX_2]_2$ (M = Co, Rh; X = Cl, I) with Na_2NCN. We have also investigated into the reactivities of coordinated NO in early and late heterobimetallic (ELHB) complexes and shown that the terminally bound NO ligand at a Rh-W bimetallic core undergoes unprecedented O-methylation.

VIII-D-1 Syntheses and Properties of NCN-Bridged Tri- and Tetranuclear Complexes of Cobalt and Rhodium

TAKAHATA, Keiichi[1]; IWADATE, Noriyuki[1]; KAJITANI, Hidenobu[2]; TANABE, Yoshiaki[1]; ISHII, Youichi[3]
([1]Chuo Univ.; [2]Univ. Tokyo; [3]IMS and Chuo Univ.)

[*J. Organomet. Chem.* in press]

The reaction of $[Cp^*CoI_2]_2$ with 2 equiv of Na NCNH affords the 16-membered macrocyclic NCNH-bridged tetracobalt(III) complex $[Cp^*CoI(\mu_2\text{-NCNH-}N,N')]_4$ (**1a**), while that with 2 equiv of Na_2NCN yields the C_3-elongated cubane-like NCN-bridged tetracobalt(III) complex $[Cp^*Co(\mu_3\text{-NCN-}N,N,N')_3(CoCp^*)_3(\mu_3\text{-NCN-}N,N,N)]$ (**2a**). Treatment of $[Cp^*RhCl_2]_2$ with 2 equiv of NaNCNH gives the C_3-elongated cubane-like tetrarhodium(III) complex $[Cp^*Rh(\mu_3\text{-NCN-}N,N,N')_3(RhCp^*)_3(\mu_3\text{-NCN-}N,N,N)]$ (**2b**) *via* the macrocyclic complex $[Cp^*RhCl(\mu_2\text{-NCNH-}N,N')]_4$ (**1b**) (Figure 1). On the other hand, the reaction of $[Cp^*Co\ Cl]_2$ with Na_2NCN affords the anionic bis(NCN)-capped tricobalt(II) complex $Na[(Cp^*Co)_3(\mu_3\text{-NCN-}N,N,N)_2]$. The molecular structures of complexes **1a**·CH_2Cl_2 and **2b**·$2C_6H_6$ have been confirmed by X-ray analyses. The electrochemical properties of these types of NCN-bridged group 9 metal complexes have also been examined.

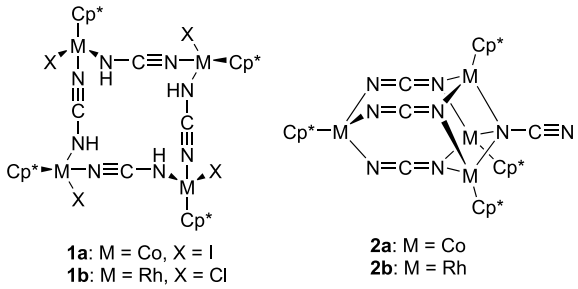

Figure 1. Structures of NCN-bridged Co and Rh tetranuclear complexes.

VIII-D-2 Electrophilic O-Methylation of a Terminal Nitrosyl Ligand Attained by Early–Late Heterobimetallic Effect

ARASHIBA, Kazuya[1]; MATSUKAWA, Shoji[2]; KUWATA, Shigeki[3]; TANABE, Yoshiaki[1]; IWASAKI, Masakazu[4]; ISHII, Youichi[5]
([1]Chuo Univ.; [2]Univ. Tokyo; [3]Tokyo Tech; [4]Saitama Inst. Tech.; [5]IMS and Chuo Univ.)

[*Organometallics* **25**, 560–562 (2006)]

The reaction of the group 9 bis(hydrosulfido) complexes $[Cp^*M(SH)_2(PMe_3)]$ (M = Rh, Ir) with the group 6 nitrosyl complexes $[Cp^*M'Cl_2(NO)]$ (M' = Mo, W) in the presence of NEt_3 affords a series of the bis(sulfido)-bridged early-late heterobimetallic (ELHB) complexes $[Cp^*M(PMe_3)(\mu\text{-S})_2M'(NO)Cp^*]$ (M = Rh, Ir; M' = Mo, W). These complexes show one strong IR absorption assignable to the NO stretching around 1500 cm^{-1}. Interestingly, this ν(NO) value is 100 cm^{-1} smaller than that of the mononuclear thiolato complex $[Cp^*W(NO)(SPh)_2]$. This unusual IR absorption is attributable to the influx of electrons to the group 6 metal center through the M(III) → M'(II) dative bond. The electron rich nature of the dinuclear complexes is reflected in its reactivities. Upon treatment of the Rh–W complex with MeOTf, the oxygen atom of the terminal nitrosyl ligand is readily methylated to form the methoxyimido complex $[Cp^*Rh(PMe_3)(\mu\text{-S})_2W(NOMe)Cp^*]^+$, while methylation of the Rh–Mo complex results in S-methylation, giving the methanethiolato complex $[Cp^*Rh(PMe_3)(\mu\text{-SMe})(\mu\text{-S})Mo(NO)Cp^*]^+$ (Scheme 1).

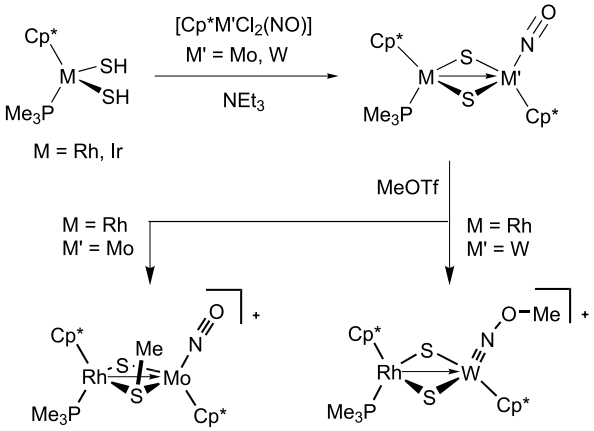

Scheme 1.

VIII-E Transition Metal Cluster Chemistry

VIII-E-1 Metathesis Approach to Linkage of Two Tetraplatinum Cluster Units: Synthesis, Characterization, and Dimerization of $[Pt_4(\mu\text{-}OCOCH_3)_7(\mu\text{-}OCO(CH_2)_nCH{=}CH_2)]$ (n = 0–3)

MASHIMA, Kazushi[1]; OHASHI, Masato[2]; YAGYU, Akihiro[2]; XU, Qinghong[2]
([1]IMS and Osaka Univ.; [2]Osaka Univ.)

Reaction of $[Pt_4(\mu\text{-}OCOCH_3)_8]$ (**1**) with 1 equiv of acrylic acid led to the selective mono-substitution of one of the four *in*-plane acetates in **1**, affording $[Pt_4(\mu\text{-}OCOCH_3)_7(\mu\text{-}OCOCH{=}CH_2)]$ (**2a**) (eq. 1), whereas treatment with excess amounts of acrylic acid resulted in a full-substitution of four *in*-plane acetates, yielding $[Pt_4(\mu\text{-}OCOCH_3)_4(\mu\text{-}OCOCH{=}CH_2)_4]$ (**3**) (Figure 1). Similarly, mono-substituted heptaacetate complexes $[Pt_4(\mu\text{-}OCOCH_3)_7\{\mu\text{-}OCO(CH)_nCH{=}CH_2\}]$ (**2b-d**: n = 1–3) were prepared. These complexes **2a-d** seem to be a suitable precursor for linkage of the Pt_4 units. Catalytic intermolecular coupling reactions of **2c** and **2d** assisted by Grubbs' catalysts gave the desired dimers $[\{Pt_4(\mu\text{-}OCOCH_3)_7\}_2\{\mu\text{-}OCO(CH_2)_nCH{=}CH(CH_2)_n(\mu\text{-}OCO)\}]$ (**6c**: n = 2; **6d**: n = 3) (eq. 2), while metathesis reactions using complexes **2a** and **2b** did not proceed under the same catalytic condition.

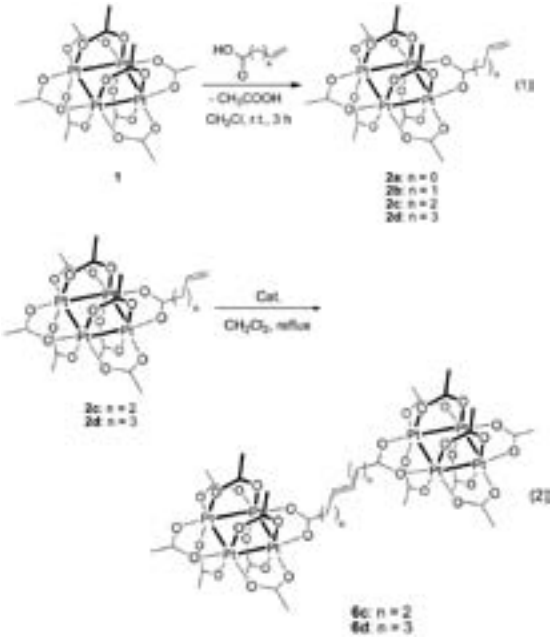

VIII-E-2 Hexapalladium Cluster: Unique Reaction of Cyclic $Pd_3(CNC_6H_3Me_2\text{-}2,6)_6$ and Linear $[Pd_3(CNC_6H_3Me_2\text{-}2,6)_8]^{2+}$

MASHIMA, Kazushi[1]; YI, Jianjun[2]; YAMAGATA, Tsuneaki[2]; OHASHI, Masato[2]
([1]IMS and Osaka Univ.; [2]Osaka Univ.)

Polynuclure clusters with metal–metal bonds have attracted research interest due to their fundamental aspect as surface model of heterogeneous catalyst, as well as potential applications as electrochemical, photoelectric and magnetic mareials. Among them, di- and trinuclear complexes with metal–metal bonds have been well documented, and have been used as starting materials to construct new clusters with high nuclearity. Many di- or trinuclear palladium and platinum complexes with isocyanide ligands have been formed by electrochemical preparation as well as by redox reactions between metal ions in different formal oxidation states. It has been reported that dicationic dinuclear palladium isocyanide complex $[Pd_2L_6]^{2+}$ (L = isocyanide) with d^9 configuration reacted with Pd^0L_x sources with d^{10} configuration such as cyclic trinuclear palladium isocyanide complex $(Pd^0L_2)_3$ resulted in the selective formation of dicationic linear trinuclear palladium complex $[Pd_3L_8]^{2+}$, where Pd(0) formally inserted into Pd–Pd bond of $[Pd_2L_6]^{2+}$ (eq. 1). However, additional reaction of $[Pd_3L_8]^{2+}$ with "Pd^0L_2" species has not been reported.

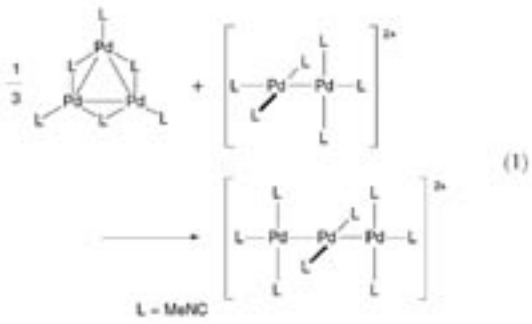

Recently we used 2,6-dimethylphenyl-isocyanide as the homoleptic ligand to develop this reaction by preparing $[Pd_3(CNC_6H_3Me_2\text{-}2,6)_8][PF_6]_2$ (**3**) from $[Pd(CNC_6H_3Me_2\text{-}2,6)_2]_3$ (**1**) and $[Pd_2(CNC_6H_3Me_2\text{-}2,6)_6][PF_6]_2$ (**2**). Herein we reported that the additional reaction of **3** and **1** selectively afforded a dicationic hexanuclear palladium complex $[Pd_6(CNC_6H_3Me_2\text{-}2,6)_{10}][PF_6]_2$ (**4**) (eq. 2, L = 2,6-$Me_2C_6H_3NC$). The crystal structure of the complex **4** was determined by X-ray crystallography and spectroscopic analysis.

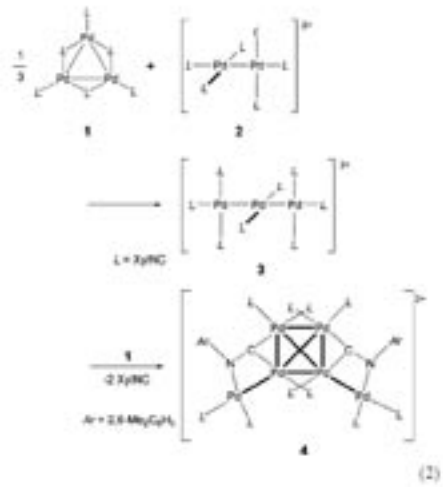

VIII-F Synthesis of Transition Metal Catalysts for Organic Transformations

VIII-F-1 Oxidative Addition of RCO_2H and HX to Chiral Diphosphine Complexes of Iridium(I): Convenient Synthesis of Mononuclear Halo-Carboxylate Iridium(III) Complexes and Cationic Dinuclear Triply Halogen-bridged Iridium(III) Complexes and Their Catalytic Performance in Asymmetric Hydrogenation of Cyclic Imines and 2-Phenylquinoline

MASHIMA, Kazushi[1]; YAMAGATA, Tsuneaki[2]; TADAOKA, Hiroshi[2]; NAGATA, Mitsuhiro[2]; HIRAO, Tsukasa[2]; RATOVELOMANANA-VIDAL, Virginie[3]; GENET, Jean Pierre[3]
([1]IMS and Osaka Univ.; [2]Osaka Univ.; [3]Ecole Natl. Supérieure Chim. Paris)

Mononuclear iridium(III) complexes of the general formula $IrX(H)(O_2CR)$[(*S*)-binap] (**2**: R = CH_3; **3**: R = Ph; **4**: R = $C_6H_4CH_3$-*p*; **a**: X = Cl; **b**: X = Br; **c**: X = I) were prepared by one-pot reaction of $[Ir(\mu\text{-}X)(cod)]_2$ with two equiv of (*S*)-BINAP [= 2,2'-bis(diphenylphosphino)-1,1'-binaphthyl] and an excess of the corresponding carboxylic acid in toluene. The structure of (*S*)-**2-4** bearing an (*S*)-BINAP was confirmed to be OC-6-23-A (Λ-conformation) by X-ray analysis of (*S*)-**4a-c**. In this reaction, an iridium(I) complex $\{Ir(\mu\text{-}Cl)[(S)\text{-binap}]\}_2$ [(*S*)-**5a**] and pentacoordinated iridium(I) complexes IrX(cod)[(*S*)-binap] [(*S*)-**7b**: X = Br; (*S*)-**7c**: X = I] were generated prior to the oxidative addition of carboxylic acid. Cationic dinuclear iridium(III) complexes of the general formula $[\{Ir(H)[(S)\text{-binap}]\}_2(\mu\text{-}X)_3]X$ [(*S*)-**8**: **a**: X = Cl; **b**: X = Br; **c**: X = I] were prepared and their cationic bifacial octahedral dinuclear structure was characterized by spectral data and combustion analysis. The anionic portion of these complexes could be replaced by $NaPF_6$, leading to the corresponding PF_6 salts, $[\{Ir(H)[(S)\text{-binap}]\}_2(\mu\text{-}X)_3]PF_6$ [(*S*)-**8**: **d**: X = Cl; **e**: X = Br; **f**: X = I]. Iodo-acetate complexes of *p*-TolBINAP (= 2,2'-bis(di-4-tolylphosphino)-1,1'-binaphthyl) [(*S*)-**9c**] and SYNPHOS [= 2,2',3,3'-tetrahydro(5,5'-bi-1,4-benzodioxin)-6,6'-diyl]bis(diphenylphosphine)] [(*S*)-**10c**] were also prepared according to the method used for the BINAP complex (*S*)-**2c** and were characterized spectroscopically. Cationic dinuclear complexes of *p*-TolBINAP [(*S*)-**11c**] and SYNPHOS [(*S*)-**12c**] were also generated. Using these complexes, the effect of halide variation was studied by asymmetric hydrogenation of 2-phenylpyrrolidine and 2-phenyl-4,5,6,7-tetrahydro-3H-azepine along with 2-phenylquinoline, and the results indicated that iodide complexes were better catalyst precursors for catalytic activity than the corresponding chloride and bromide complexes, but were not superior in enantioselectivity.

VIII-G Early Transition Metal Complexes

VIII-G-1 Synthesis, Structure, and Reactivity of Tantalum and Tungsten Homoenolate Complexes

MASHIMA, Kazushi[1]; TSURUGI, Hayato[2]; OHNO, Takashi[2]; YAMAGATA, Tsuneaki[2]
([1]IMS and Osaka Univ.; [2]Osaka Univ.)

Preparation and characterization of homoenolate complexes of tantalum, $Cp^*Cl_3Ta(CH_2CR^1{}_2C(=O)OR^2)$ (**1a** : R^1 = H, R^2 = Et; **1b** : $R^1 = R^2$ = Me; **1c** : R^1 = Me, R^2 = $C_6H_4CH_3$-4), and tungsten, $(Xyl\text{-}N=)Cl_3W(CH_2CH_2C(=O)OEt)$ (**7**), using zinc homoenolate reagents are described. Intramolecular coordination of the carbonyl moiety to the metal center in these complexes was confirmed by their NMR and IR spectroscopy together with X-ray analyses of **1a** and **1b**. The insertion reaction of isocyanide into the metal carbon bond of **1a** and **7**, respectively, resulted in the formation of a diazametallacycle, $Cp^*Cl_3Ta[N(Xyl)\text{-}C(=C=N\text{-}Xyl)\text{-}C(CH_2CH_2CO_2Et)=N\text{-}Xyl]$ (**3a**), which possesses a metallacyclic structure with an exocyclic ketene-imine moiety, and an η^2-iminoacyl tungsten complex, $(Xyl\text{-}N=)W\{C(=N\text{-}Xyl)CH_2CH_2CO_2Et\}(CNXyl)Cl_3$ (**8**). The β-proton of the homoenolate moiety of **1a** was selectively deprotonated by $KN(SiMe_3)_2$ to afford an η^4-ethyl acrylate complex, $Cp^*Cl_2Ta(\eta^4\text{-ethyl acrylate})$ (**4**). In the case of complex **1b**, in which the β-positions were protected by dimethyl substituents, reaction with the dilithium salt of diazadiene afforded a tantalalactone complex **5**. The addition of $Al(C_6F_5)_3$ to **5** afforded a novel zwitterionic complex **6**, in which $Al(C_6F_5)_3$ coordinated to the exocyclic carbonyl oxygen of the tantalalactone.

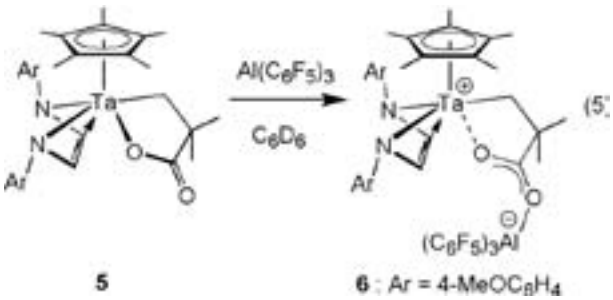

5 **6** : Ar = 4-$MeOC_6H_4$

VIII-H Creation of Novel Functional Nano Materials Based on Proton-Coupled Electronic Properties

Dynamics of molecules and ions in "coordination nano-space" are acted by characteristic nano-fields such as intermolecular interaction, coulomb interaction, catalytic action, *etc*. This project is to reveal a basic principle of an unusual nano-field acting on coordination space, and to create the nano space where the energy conversions can be easily operated. In particular, we aim at the construction of coordination nano space system which is able to control a series of energy operations such as generation, separation, storage, material conversion of an energy molecule H_2, or electron/ion transport. In this year, we have explored a novel hydrogen-energy functional coordination nano-space by using proton-coupled redox and electron-proton interaction. In the present project, we will create new 1) hydrogen-storage nano-materials, 2) highly proton-conductive coordinatiom polymers, 3) highly electron-proton conductive matrerials, *etc*.

VIII-H-1 Most Stable Metallic Phase of the Mixed-Valence MMX-Chain, $Pt_2(dtp)_4I$ (dtp: $C_2H_5CS_2^-$) in Purely *d*-Electronic Conductors Based on the Transition-Metal Complex

OTSUBO, Kazuya[1]; KOBAYASHI, Atsushi[1]; KITAGAWA, Hiroshi[2]; HEDO, Masato[3]; UWATOKO, Yoshiya[3]; SAGAYAMA, Hajime[4]; WAKABAYASHI, Yusuke[4]; SAWA, Hiroshi[4]
([1]Kyushu Univ.; [2]IMS and Kyushu Univ.; [3]Univ. Tokyo; [4]KEK-PF)

[*J. Am. Chem. Soc.* **128**, 8140–8141 (2006)]

The electrical resistivity and X-ray oscillation photograph measurements for an MMX-Chain complex, $Pt_2(dtp)_4I$ (dtp = $C_2H_5CS_2^-$) under high pressure were performed. We observed the most stable metallic phase (T_{MI} = 70 K, under 2.2 GPa) in the 1-D purely *d*-electronic conductors and pressure-induced metal–insulator transition including structural phase transition at 3.0 GPa.

VIII-H-2 Direct Determination of Low-Dimensional Structures: Synchrotron X-Ray Scattering on One-Dimensional Charge-Ordered MMX-Chain Complexes

WAKABAYASHI, Yusuke[1]; KOBAYASHI, Atsushi[2]; SAWA, Hiroshi[1]; OHSUMI, Hiroyuki[3]; IKEDA, Naoshi[3]; KITAGAWA, Hiroshi[4]
([1]KEK-PF; [2]Kyushu Univ.; [3]JASRI; [4]IMS and Kyushu Univ.)

[*J. Am. Chem. Soc.* **128**, 6676–6682 (2006)]

A powerful method to determine the hidden structural parameters in functional molecules has been developed. Local valence arrangements that dominate the material properties are sometimes not three-dimensionally ordered. This method that comprises diffuse X-ray scattering and resonant X-ray scattering is suitable in such cases. Using this method, we present clear evidence of the low-dimensional valence arrangement in two halogen-bridged one-dimensional metal complexes, so-called MMX chains. This family allows us to control many physical and structural parameters by chemical substitution of bridging halogen, counterions, or metal ions, and one of our samples carries an unusual metallic phase. It is demonstrated with this complex that the present method makes it possible to have microscopic insight to low-dimensionally ordered systems.

VIII-H-3 Pressure-Induced Metal–Semiconductor–Metal Transitions in an MMX-Chain Complex, $Pt_2(C_2H_5CS_2)_4I$

KOBAYASHI, Atsushi[1]; TOKUNAGA, Aya[2]; IKEDA, Ryuichi[2]; SAGAYAMA, Hajime[3]; WAKABAYASHI, Yusuke[3]; SAWA, Hiroshi[3]; HEDO, Masato[4]; UWATOKO, Yoshiya[4]; KITAGAWA, Hiroshi[5]
([1]Kyushu Univ.; [2]Univ. Tsukuba; [3]KEK-PF; [4]Univ. Tokyo; [5]IMS and Kyushu Univ.)

[*Eur. J. Inorg. Chem.* 3567–3578 (2006)]

The electrical conductivity and X-ray diffraction measurements under high pressure up to 2.5 GPa were performed for a highly-conductive halogen-bridged binuclear-metal mixed-valence complex (the so-called MMX chain), $Pt_2(C_2H_5CS_2)_4I$. It exhibited pressure-induced metal-semiconductor-metal transitions at 0.5 and 2.1 GPa. The X-ray diffuse scatterings were observed at $k = n + 0.5$ (n: integer) under ambient pressure, which are derived from the charge-density-wave (CDW: $\cdots Pt^{2+}–Pt^{2+}\cdots I–Pt^{3+}–Pt^{3+}–I\cdots$) fluctuation in the MMX chain. Above 0.5 GPa where the pressure-induced metal-semiconductor transition occurred, these scatterings disappeared. The electronic phases under high pressure (P) were found to be attributable to the metallic averaged-valence state (AV: $–Pt^{2.5+}–Pt^{2.5+}–I–Pt^{2.5+}–Pt^{2.5+}–I–$) with CDW fluctuation for $P < 0.5$ GPa, semiconducting charge-polarization state (CP: $\cdots Pt^{2+}–Pt^{3+}–I\cdots Pt^{2+}–Pt^{3+}–I\cdots$) for $0.5 < P < 2.1$ GPa, and metallic AV state for $P > 2.1$ GPa. The electronic state of $Pt_2(C_2H_5CS_2)_4I$ is very sensitive to pressure, implying that phase competition among the CP, CDW and AV phases is present in the MMX chain.

VIII-H-4 Synthesis of a One-Dimensional Metal-Dimer Assembled System with Interdimer Interaction, $M_2(dtp)_4$ (M = Ni, Pd; dtp = Dithiopropionato)

KOBAYASHI, Atsushi[1]; KOJIMA, Takahiko[1];

IKEDA, Ryuichi[2]; KITAGAWA, Hiroshi[3]
([1]Kyushu Univ.; [2]Univ. Tsukuba; [3]IMS and Kyushu Univ.)

[*Inorg. Chem.* **45**, 322–327 (2006)]

A metal-dimer assembled system, $M_2(dtp)_4$ (M = Ni, Pd; *dtp* = dithiopropionate, $C_2H_5CS_2^-$) was synthesized and analyzed by X-ray single-crystal diffraction method, UV-Vis-Near-IR of solutions and solid state diffuse reflectance spectroscopies, and electrical conductivity measurement. The structures exhibit one-dimensional metal-dimer chains of $–M_2(dtp)_4–M_2(dtp)_4–M_2(dtp)_4–$ with moderate interdimer contact. These complexes are semiconducting or insulating, which is consistent with the fully filled d_z^2 band of $M^{II}(d^8)$. Interdimer metal–metal distances were 3.644(2) Å in $Ni_2(dtp)_4$ and 3.428(2) Å in $Pd_2(dtp)_4$, each of which is marginally longer than twice the van der Waals radius of the metal. Interdimer charge-transfer transitions were nevertheless observed in diffuse reflectance spectra. The origin of this transition is considered to be due to an overlap of two adjacent d_{σ^*} orbitals which spread out more than d_z^2 orbital due to the antibonding d_{σ^*} character of the $M(d_z^2)–M(d_z^2)$. The $Ni_2(dtp)_4$ exhibited an interdimer charge transfer band at relatively low energy region, which is derived from the Coulomb repulsion of $3d_{\sigma^*}$ orbital of Ni.

VIII-H-5 Galvanostatic Transient Studies on Copper Coordination Polymer under Hydrogen Absorption

FUJISHIMA, Musashi[1]; ENYO, Michio[2]; KANDA, Seiichi[3]; IKEDA, Ryuichi[4]; KITAGAWA, Hiroshi[5]
([1]Kinki Univ.; [2]Hokkaido Univ.; [3]Univ. Tokushima; [4]Univ. Tsukuba; [5]IMS and Kyushu Univ.)

[*Chem. Lett.* **35**, 546–547 (2006)]

Hydrogen electrode reaction (HER) was investigated for a copper coordination polymer, catena-μ-*N*,*N*'-bis (hydroxyethyl)dithiooxamidatocopper(II) (CuCP) by galvanostatic transient measurements using a palladium cathode. Individual steps in the Volmer–Tafel reaction were successfully observed for the colloidal CuCP in alkaline solution under hydrogen absorption. The Volmer step was found to be promoted with CuCP and its hydrogen-absorbed polymer (CuCPH) from shorter decay times in transient curves and smaller overpotentials in Tafel plots. In contrast, the inhibition of the Tafel step was observed, which is due to the larger overpotentials. Difference in reducibility between the polymers and plausible reduction mechanisms is discussed.

VIII-I Development of Metal-Cojugated Redox Systems in Metal-Dioxolene Complexes and Electrochemical Activation of Water Ligand

Dioxolenes function as a versatile electron-acceptor and electron-donor through the reversible two-electron redox reactions among the three oxidation states of catechol (Cat), semiquinone (SQ), and quinone (Q). A variety of metal–dioxolene complexes has appeared and the unique metal-conjugated electronic interaction has been extensively investigated. The ruthenium–terpyridine–dioxolene complexes exhibit the reversible two-electron redox behavior derived from a resonance hybrid between the metal center and the dioxolene ligand. In the ruthenium–dioxolene complex, its aqua ligand undergoes the electrochemical activation to generate a novel ruthenium–oxo bond. Fabrication of a water-soluble ruthenium–terpyridine complex having a strongly electron-withdrawing dioxolene is a particularly urgent target for the future applications as an electrochemical catalyst utilizing water molecules.

VIII-I-1 Synthesis of a Water-Soluble Ruthenium–Terpyridine–Dioxolene and the Electrochemical Activation of Water Molecules

KURIHARA, Masato[1]; MIURA, Yasutaka[2]; SAKAMOTO, Masatomi[2]; WADA, Tohru; TANAKA, Koji

([1]IMS and Yamagata Univ.; [2]Yamagata Univ.)

A ruthenium-terpyridine-dioxolene complex having a chloro ligand was synthesized using 4-nitrocatechol. The dioxolene complex, $[Ru^{II}Cl(NO_2\text{-}SQ)(terpy)]$ was transformed to a hydroxo complex, $[Ru^{II}(OH)(NO_2\text{-}SQ)(terpy)]$ (**1**) by elimination of the chloro ligand with Ag^+ in acetone/water, where terpy and NO_2-SQ are 2,2':6',2"-terpyridine and 4-nitrobenzosemiquinone, respectively. The hydroxo complex, **1** is soluble in water, unlike the chloro complex. The intense near-IR absorption band of **1** is ascribable to the Ru(II) → NO_2–SQ charge transfer. Both of the complexes show two-reversible redox waves of the cyclic voltammograms (CV) in the organic solvents. Based on the electro-spectrochemical measurement, the two-redox reactions correspond to Ru(II)–NO_2–Cat ↔ Ru(II)–NO_2–SQ ↔ Ru(III)–NO_2–SQ (Ru(II)–NO_2–Q). The UV-Vis-near-IR absorption spectrum and CV of **1** are significantly changed depending on pH in water. In pH 12, a catalytic current is observed around 0.7 V *vs*. Ag/AgCl. When we suppose that oxygen molecules are evolved catalytically at the oxidation potential, an electrocatalytic cycle can be proposed, as shown in Scheme 1.

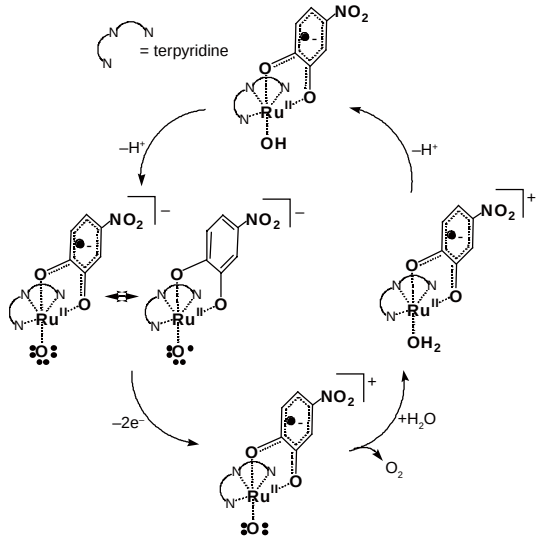

Scheme 1. The electrocatalytic cycle.

VIII-J Syntheses, Structures, and Redox Properties of New Multinuclear Coordination Materials with Metallocene Units

Coordination materials with metallocene are of interest for creations of new redox-active crystalline solids, in which ferrocene moieties have mainly been utilized as the redox-active units. Because other metallocene such as ruthenocene and cobaltocene are known to show quite different potentials compared to ferrocene units, coordination materials with such metallocene units in the framework are promising compounds that show different redox properties compared with those for ferrocene units. Nevertheless the coordination materials with their metallocene units are still unexplored. This project proceeds synthesis, and characterizations of new coordination materials with metallocene and metallocenium units with dicarboxylate 1,1'-dicarboxylate. These studies show that the compounds obtained demonstrate unique dynamics depending on the free rotations of the Cp–M–Cp rotations as well as the redox properties based on the metallocene units.

VIII-J-1 Synthesis of Coordination Polymers with Cobaltocenium and Rhodocenium Units

KONDO, Mitsuru[1]; HAYAKAWA, Yuri[2]; UNOURA, Kei[3]; KAWAGUCHI, Hiroyuki
([1]IMS and Shizuoka Univ.; [2]Shizuoka Univ.; [3]Yamagata Univ.)

Four new redox-active crystalline coordination polymers with cobaltocenium-1,1'-dicarboxylate (ccdc) have been synthesized and characterized. The crystalline materials, $[Cu(ccdc)_2]\cdot 2MeOH$ (**1**) and $[M(ccdc)_2]\cdot 2DMF$ (M = Co (**2**), Zn (**3**)) were obtained by a treatment of Hccdc and Hrcdc with the corresponding $M(CH_3COO)_2$. Because of the charge balance, ccdc acts as monoanionic dicarboxylate ligand, yielding $M(ccdc)_2$ type compounds. Crystal structural analyses clearly demonstrated that these compounds have two-dimensional structure (Scheme 1). The free rotations based on the crystal structures are revealed for these compounds.

The high redox properties of **1**-**4** based on the ccdc components were characterized by solid-state cyclic voltammogram (CV).

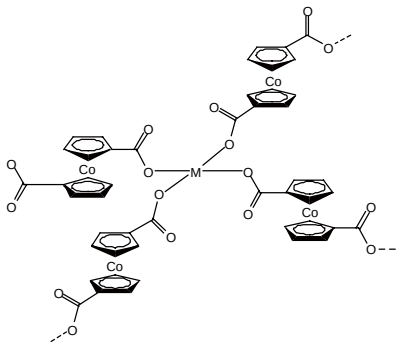

Scheme 1.

The quasi reversible redox waves ascribed to the Co(III)/Co(II) couple of the ccdc centers are observed at –933 and –831 mV (*vs*. SCE) in 1,2-dichloroethane media for **1** and **2**, respectively. Although these potentials change depending on the electrolyte solvents used for the measurements, the orders (**1** < **2** < **3**) of the potentials are retained. The correlations between the reduction processes and the LUMO levels were revealed by preliminary molecular orbital calculation.

VIII-J-2 Synthesis of Coordination Networks with Ruthenocdene Units

KONDO, Mitsuru[1]; KOBAYASHI, Yuko[2]; KAWAGUCHI, Hiroyuki
([1]IMS and Shizuoka Univ.; [2]Shizuoka Univ.)

As a ruthenocene assembled complex, $[(H_2bpe)(rcdc)]$ (bpe = 4,4'-bipyridylethylene, rcdc = ruthenocene-1,1'-dicarboxylate) was prepared and structurally characterized. Treatment of H_2rcdc with bpe yields the compound as pale pink crystals. The carboxylate groups of the rcdc form hydrogen bonds to the protonated pyridine nitrogen atom of the bpe. These interactions yield the infinite one-dimensional chain structure (Scheme 1).

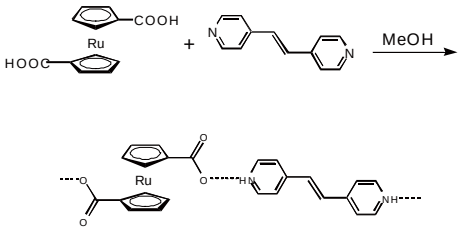

Scheme 1.